Journal of Medicinal Chemistry

Article

pubs.acs.org/jmc

New Nucleotide-Competitive Non-Nucleoside Inhibitors of Terminal Deoxynucleotidyl Transferase: Discovery, Characterization, and Crystal Structure in Complex with the Target

Roberta Costi,*[,†] Giuliana Cuzzucoli Crucitti,[†] Luca Pescatori,[†] Antonella Messore,[†] Luigi Scipione,[†] Silvano Tortorella,[†] Alessandra Amoroso,[‡] Emmanuele Crespan,[‡] Pietro Campiglia,[§] Bruno Maresca,[§] Amalia Porta,[§] Ilaria Granata,[§] Ettore Novellino,[∥] Jérôme Gouge,[⊥] Marc Delarue,[⊥] Giovanni Maga,[‡,#] and Roberto Di Santo[†,#]

[†]Dipartimento di Chimica e Tecnologie del Farmaco, Istituto Pasteur—Fondazione Cenci Bolognetti, "Sapienza" Università di Roma, P.le Aldo Moro 5, I-00185 Roma, Italy

[‡]Institute of Molecular Genetics IGM-CNR, Via Abbiategrasso 207, I-27100 Pavia, Italy

[§]Department of Pharmaceutical and BioMedical Sciences, University of Salerno, I-84084 Fisciano, Salerno, Italy

[∥]Dipartimento di Farmacia, Università di Napoli "Federico II", Via D. Montesano 49, I-80131 Napoli, Italy

[⊥]Dynamique Structurale des Macromolecules, UMR 3528, CNRS, Institut Pasteur, 25 Rue du Dr Roux, 75015 Paris, France

Supporting Information

ABSTRACT: Terminal deoxynucletidyl transferase (TdT) is overexpressed in some cancer types, where it might compete with pol μ during the mutagenic repair of double strand breaks (DSBs) through the nonhomologous end joining (NHEJ) pathway. Here we report the discovery and characterization of pyrrolyl and indolyl diketo acids that specifically target TdT and behave as nucleotide-competitive inhibitors. These compounds show a selective toxicity toward MOLT-4 compared to HeLa cells that correlate well with in vitro selectivity for TdT. The binding site of two of these inhibitors was determined by cocrystallization with TdT, explaining why these compounds are competitive inhibitors of the deoxynucleotide triphosphate (dNTP). In addition, because of the observed dual localization of the phenyl substituent, these studies open the possibility of rationally designing more potent compounds.

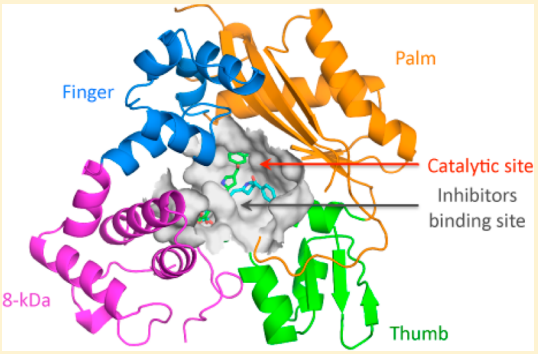

INTRODUCTION

A common feature to all polymerases is to act in a template-dependent manner so that they require a DNA strand to direct the polymerization process.[1] However, this mechanism differs for just one type of DNA polymerizing enzyme, called terminal deoxynucleotidyl transferase (TdT)[2,3] which can incorporate nucleotides in a template independent manner without needing a template strand.

The preferred substrate for this enzyme are 3′ protruding ends, but it is also able to add nucleotides to blunt and 3′-recessed ends of double strand DNA fragments. TdT was one of the first DNA polymerases identified in mammalian cells[4] first from thymus and later in bone marrow.[5]

The main role of this enzyme is in the V(D)J recombination process, where the TdT randomly adds nucleotides to single-stranded DNA,[6−8] increasing the antibody repertoire diversity. For this reason TdT plays a fundamental role in the development of the vertebrate's immune system.

TdT is expressed in B cells during development, before D-J rearrangement, and it ceases before the expression of Ig light chains. The premature introduction of TdT activity in mice during its fetal and neonatal life, when such TdT activity is absent, results in an altered ability to make protective antibodies.[6,9] TdT is overexpressed in some cancer types, where it might compete with pol μ driving the mutagenic repair of double strand breaks (DSBs) through the nonhomologous end joining (NHEJ) pathway. However, NHEJ by TdT is very error-prone, contributing to mutagenesis of tumor cells.

Numerous clinical studies showed that altered expression levels and activity of TdT have a critical role for cancer development and might worsen the response to anticancer chemotherapy.[10] TdT overexpression has been observed in B and T cell acute lymphocytic leukemia (ALL) and acute myelocitic leukemia (AML).[10−12] Generally, the TdT expression in AML patients is quite variable, whereas in ALL patients TdT is overexpressed in about 90% of cases, and this overexpression correlates to poor prognosis and response to chemotherapy.[13]

The correlation between the high TdT activity and the malignancy of ALL, and the lack of TdT in normal adult tissues,

Received: July 5, 2013
Published: August 22, 2013

further increased the interest in developing selective inhibitors against TdT as chemotherapeutic agents against leukemia. One such compound, developed by McCaffrey and colleagues, is cordycepin,[14] a nucleoside analogue (3′deoxyadenosine) that can inhibit single stranded DNA synthesis by TdT in vitro. However, cordycepin has some serious side effects, due to its inhibition of different enzymes involved in the cellular metabolism, and cannot be considered a selective TdT inhibitor.[15,16] Consequently, researchers' attention has been directed toward the synthesis of more selective TdT inhibitors. We have previously characterized compounds **2k** and **4e** (Figure 1), two

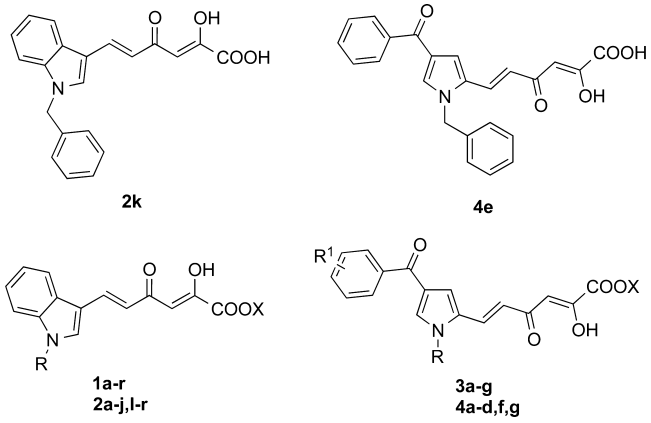

Figure 1. Hit compounds **2k** and **4e** and the newly designed diketohexenoic derivatives **1a−r**, **2a−j,l−r**, **3a−g**, and **4a−d,f,g**.

non-nucleoside inhibitors of mammalian TdT belonging to the diketo acid class, which showed a strong cytotoxic effect against the TdT-positive leukemia cell line MOLT-4, compared to the TdT-negative cell lines derived from cervical cancer, HeLa.[17] However, **2k** and **4e** were also able to inhibit the template-independent activity of the cellular DNA polymerase (pol) λ, belonging, as TdT, to the DNA pol family X. Starting from these results, we have undertaken a screening of non-nucleoside compounds to find more selective TdT inhibitors.

In this study we describe the synthesis and characterization of novel diketohexenoic acid derivatives **1a−r**, **2a−j,l−r**, **3a−g**, and **4a−d,f,g** designed as analogues of the previously described hits **2k** and **4e**, which specifically target TdT activity and show interesting anticancer properties (Figure 1). In addition, the crystal structures of TdT in complex with **4b** and **4c** were determined at a resolution of 2.4−2.6 Å, allowing the unambiguous identification of the interacting site and providing the basis for the first rational design of further TdT inhibitors. Indeed, these crystal structures, as well as the existing crystal structures of TdT, pol λ, and pol μ in complex with their natural substrates,[18−20] can be used to devise better and more specific inhibitors.

RESULTS

Synthesis. Indole derivatives **1a−r** and **2a−r** were synthesized as reported in Scheme 1. Aldehydes **5a−p,s,t** were condensed with acetone in the presence of 5 N NaOH. The enones **6a−r** that formed were reacted with diethyl oxalate in basic conditions (NaOEt) to give diketo esters **1a−r** that were finally hydrolyzed with 1 N NaOH to afford the corresponding acids **2a−r**.

Aldehydes **5a−p,s,t** were obtained as described in Scheme 2. Indole-3-carboxaldehyde was alkylated with the appropriate alkyl halide using NaH as a base to give alkyl derivatives **5a−g,k-o,q** or arylated with the appropriate arylboronic acid following a

Scheme 1. Synthetic Route to Compounds 1a−r and 2a−r[a]

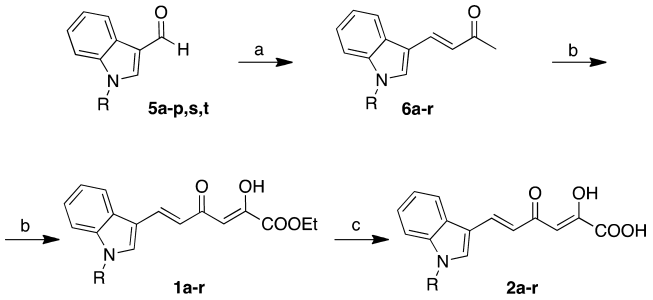

[a]Reagents and conditions: (a) 5 N NaOH, acetone, 2 nights, 50 °C; (b) diethyl oxalate, NaOEt, THF, 1.5 h, rt; (c) 1 N NaOH, THF/methanol 1:1, 30 min, rt.

Scheme 2. Synthetic Route to Compounds 5o−t[a]

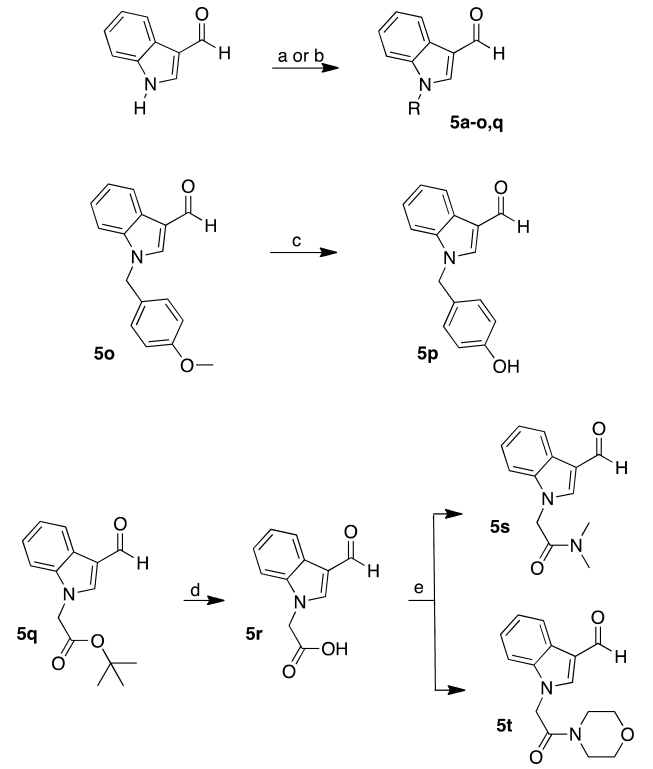

[a]Reagents and conditions: (a) DMF, NaH, alkyl halide, 1 h, room temperature; (b) arylboronic acid, cupric acetate, NMP/pyridine 1:1, microwave (60 W, 120 °C, 50 s, open vessel); (c) BBr_3, CH_2Cl_2, −45 °C, 1 h; (d) dichloromethane/trifluoroacetic acid 1:1, 16 h, room temperature; (e) morpholine or dimethylamine, HBTU, DIEA, 2 days, room temperature.

Suzuki coupling procedure to afford aryl derivatives **5h−j**. Deprotection of **5o** with BBr_3 gave the hydroxyl derivative **5p**.

Finally, aldehydes **5s,t** were obtained starting form **5q** that was deprotected with trifluoroacetic acid to give the carboxylic acid **5r**, which was transformed to amides **5s** and **5t** by activation and treatment with the appropriate amine.

Pyrrole derivatives **3a−g** and **4a−g** were synthesized as reported in Scheme 3. 1*H*-Pyrrole underwent sequential one-pot Vilsmeyer−Haack and Friedel−Crafts sequential reactions in DMF with addition of oxalyl chloride, then with aluminum trichloride and the appropriate aroyl chloride. The aldehydes **7a−e** that formed were alkylated with the appropriate benzyl

dx.doi.org/10.1021/jm4010187 | J. Med. Chem. 2013, 56, 7431−7441

Scheme 3. Synthetic Route to Compounds 3a−g and 4a−g[a]

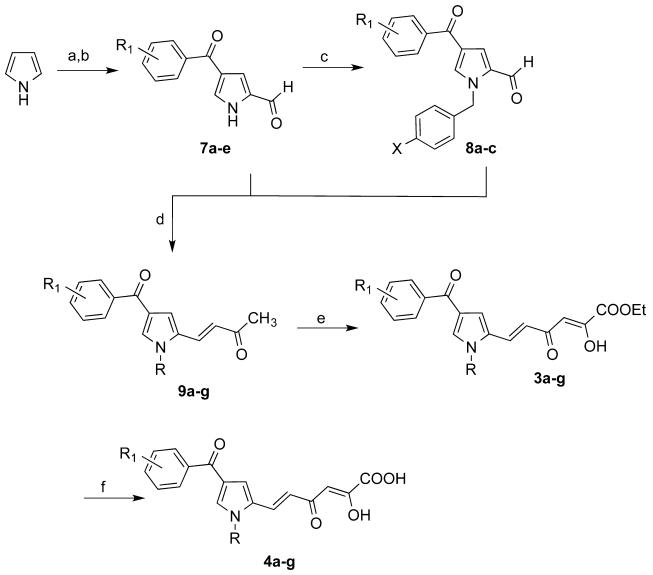

[a]Reagents and conditions: (a) DMF, oxalyl chloride, 1,2-dichloroethane, 20 min, 0 °C to room temperature; (b) $AlCl_3$, benzoyl chloride, 3 h 40 min, room temperature; (c) benzyl bromide, $Ba(OH)_2$, 5 h, 50 °C; (d) $Ba(OH)_2$, acetone, 50 °C; (e) diethyl oxalate, NaOEt, THF, 1.5 h, room temperature; (f) NaOH 1 N, THF/methanol 1:1, 30 min, room temperature.

bromide in the presence of barium hydroxide to give the N-substituted pyrroles **8a−c**. Aldehydes **7a−e** and **8a−c** were condensed with acetone to give enones **9a−g** that were reacted with ethyl oxalate to afford esters **3a−g**. Final hydrolysis of these esters led to diketo acids **4a−g**.

Biological Assay. Identification of Specific Non-Nucleoside Inhibitors of Human TdT. The newly synthesized pyrrolyl and indolyl diketohexenoic acid derivatives **1a−r**, **2a−j**,**l**-**r**, **3a−g**, and **4a−d**,**f**,**g** were tested using **2k** and **4e** as reference compounds against the family X enzymes TdT, DNA pol β, and DNA pol λ. This last enzyme was tested for its template-dependent DNA polymerase and template-independent (TdT-like) activities.

As shown in Table 1, none of the tested compounds showed significant activity against DNA pol β and only three (**1j**, **2j**, and **3b**) inhibited the template-dependent activity of DNA pol λ. Several compounds (**2b**,**d−f**,**h**,**k**,**l**,**n**, **3a**,**c**, and **4a**,**c**,**e**) inhibited both TdT and the TdT-like activity of DNA pol λ, thus confirming their specificity for template-independent DNA synthesis. Interestingly, some compounds (**2a**,**c**,**g**,**i**,**m**,**o−r**, **3b**,**d**, and **4b**,**d**,**f**,**g**) were highly selective for TdT, with no activity against DNA pol λ or β.

Non-Nucleoside Diketohexenoic Acid Derivatives Behave as Nucleotide-Competitive Inhibitors. Compounds **2p**, **4a**, and **3d** were selected for further enzymatic studies. In order to determine their exact mechanism of action, TdT inhibition was studied as a function of variable concentrations of either the nucleic acid or the nucleotide substrates. As shown in Figure 2, increasing the inhibitor concentrations also increased the apparent value of the affinity constant (K_m) for the nucleotide substrate without affecting the maximal velocity (V_{max}) of the reaction. Conversely, no effects were noted on the apparent affinity for the nucleic acid, while the V_{max} decreased as a function of the inhibitor concentrations. Collectively, these results indicated that the non-nucleoside DKA derivatives behaved as nucleotide-competitive (Nc) inhibitors. From the variation of the K_m and V_{max} values, the true inhibitory constants (K_i) for the different compounds were calculated and reported in Table 2.

The Nc Inhibitors Show Reduced Binding Affinity to the Ternary Enzymatic Complex along the Reaction Pathway Catalyzed by TdT. Similar to DNA pols, TdT is present along the reaction pathway in three distinct enzymatic forms: the free enzyme (E), the binary enzyme−nucleic acid complex (E:DNA), and the ternary enzyme−nucleic acid−nucleotide (E:DNA:dNTP) complex.

Given the competitive nature of the inhibition by DKAs with respect to the nucleotide substrate, it was of interest to assess whether the compounds tested were able to interact with all three enzymatic forms with equal affinity or not. Thus, kinetics experiments were carried out in order to determine the apparent rates of association (k_{on}) and dissociation (k_{off}) of the DKA derivatives to the three different forms of TdT. As reported in Table S1 (see Supporting Information), all compounds interacted with the free enzyme and the binary complex with DNA, with similar k_{on} and k_{off} values. On the other hand, all the compounds showed faster dissociation rates from the ternary complex with respect to the other enzymatic forms.

These data suggest that the inhibitor binding is unfavored when the nucleotide is in the active site and are consistent with the proposed nucleotide-competitive mechanism of action of these compounds.

Cytotoxic Activity of Nc Inhibitors against TdT^+ and TdT^- Tumor Cell Lines. The synthesized compounds **1k**, **2a−r**, **3a−d**, and **4a−g** were tested for their ability to suppress cellular proliferation on two different cell lines: MOLT-4, a T-lymphocytic leukemia cell line overexpressing TdT, and HeLa, a TdT negative cervical cancer cell line. As reported in Table 1, several of the compounds (**2b**,**c**,**f**,**j**,**k**,**m**,**p**, **3a−d**, and **4a**,**f**) were toxic for the TdT^+ cell line MOLT-4 but much less against the HeLa cell line. Interestingly, some of the most specific compounds toward TdT, namely, **2m**,**p**, **3d**, and **4a**, were also showing selective toxicity toward MOLT-4 with respect to HeLa cells. Compounds **3b** and **2j**, which were the only inhibitors of both TdT and the template-dependent DNA pol λ synthetic activity with similar potencies, were nonetheless selectively toxic toward MOLT-4 cells. This is consistent with the fact that DNA pol λ template-dependent activity can be substituted by its close relative DNA pol β.

Nc Inhibitors Arrest the Cell Cycle and Induce Apoptosis in TdT^+ Cancer Cells. We analyzed the effect of compounds **2b**, **3d**, and **4f** on cell cycle progression. The cytometric investigation showed a clear arrest at G1/G2 cell cycle phase of both MOLT-4 and HeLa cells treated with **2b** (30 μM) for 24 h compared to control cells. Accumulation of cells in the G1 phase increased about 20% ($p < 0.001$) with a corresponding decrease of cells in the G2 phase (about 10% lower, $p < 0.001$). This result was confirmed by Western blotting experiments that show a decrease of cyclin E expression (Figure 3 A).

Under the same conditions, treatment of MOLT-4 cells with **3d** and **4f** (30 μM) determined the arrest of the cell cycle in S phase showing cell accumulation of about 44% of cells in this phase and a decrease in G1 phase of about 30%. However, similar treatment of HeLa cells did not show any significant effect on the cell cycle progression. The arrest of cell cycle induced by **3d** and **4f** in MOLT-4 cells correlated well with a

dx.doi.org/10.1021/jm4010187 | J. Med. Chem. 2013, 56, 7431−7441

Table 1. Inhibitory Activity of Compounds 1a−r, 2a−r, 3a-g, and 4a−g against Human DNA Polymerases and TdT and Their Activities in Cell Based Assays

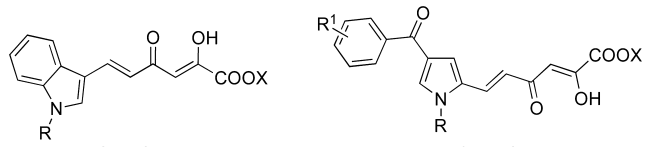

1a-r, 2a-r 3a-g, 4a-g

				enzymatic assay,[a] ID_{50} (μM)			cell-based assay,[b] IC_{50} (μM)		
compd	R^1	R	X	TdT	pol λ (TdT)	pol λ (Pol)	pol β	MOLT-4[g]	HeLa[g]
1a		$(CH_2)_2CH_3$	Et	>40[f]	>40	>40	>40	nt	nt
1b		$(CH_2)_3CH_3$	Et	>40	>40	>40	>40	nt	nt
1c		$(CH_2)_2CH(CH_3)_2$	Et	>40	>40	>40	>40	nt	nt
1d		$CH{=}CHCH_3$	Et	>40	>40	>40	>40	nt	nt
1e		$CH_2CH{=}CHCH_3$	Et	>40	>40	>40	>40	nt	nt
1f		$CH{=}C(CH_3)_2$	Et	>40	>40	>40	>40	nt	nt
1g		$CH_2CH(CH_3){=}CH$	Et	>40	>40	>40	>40	nt	nt
1h		Ph[c]	Et	>40	>40	>40	nt	nt	nt
1i		4-OH-Ph[c]	Et	>40	>40	>40	>40	nt	nt
1j		4-Cl-Ph[c]	Et	>40	>40	6	>40	nt	nt
1k		Bn[d]	Et	>40	>40	>40	>40	>40	>40
1l		4-F-Bn[d]	Et	>40	>40	>40	>40	nt	nt
1m		4-Cl-Bn[d]	Et	40 ± 4	>40	>40	>40	nt	nt
1n		4-CN-Bn[d]	Et	>40	>40	>40	>40	nt	nt
1o		4-OCH_3-Bn[d]	Et	>40	>40	>40	>40	nt	nt
1p		4-OH-Bn[d]	Et	40 ± 4	>40	>40	>40	nt	nt
1q		$CH_2(C{=}O)N(CH_3)_2$	Et	>40	>40	>40	>40	nt	nt
1r		$CH_2(C{=}O)$Morph[e]	Et	>40	>40	>40	>40	nt	nt
2a		$(CH_2)_2CH_3$	H	3.1 ± 0.1	>40	>40	>40	50 ± 5	>40
2b		$(CH_2)_3CH_3$	H	26 ± 1	>40	>40	>40	30 ± 2	30
2c		$(CH_2)_2CH(CH_3)_2$	H	16.3 ± 0.5	>40	>40	>40	20	>80
2d		$CH{=}CHCH_3$	H	33 ± 2	10 ± 0.2	>40	>40	>40	>40
2e		$CH_2CH{=}CHCH_3$	H	7.3 ± 0.3	5 ± 0.2	>40	>40	>40	>40
2f		$CH{=}C(CH_3)_2$	H	13.8 ± 0.7	9 ± 0.5	>40	>40	30 ± 2	>40
2g		$CH_2CH(CH_3){=}CH$	H	2.5 ± 0.2	40 ± 2	>40	>40	40 ± 2	40
2h		Ph[c]	H	47 ± 2	2 ± 0.1	>50	>40	>40	>40
2i		4-OH-Ph[c]	H	5.2 ± 0.5	>40	>40	>40	>40	>40
2j		4-Cl-Ph[c]	H	31 ± 0.5	>40	9	>40	27 ± 1	>40
2k		Bn[d]	H	7.9 ± 0.5	1.7 ± 0.1	>40	>40	15 ± 1	>40
2l		4-F-Bn[d]	H	10 ± 0.5	>40	>40	>40	>40	>40
2m		4-Cl-Bn[d]	H	10 ± 0.6	>40	>40	>40	19 ± 0.1	>40
2n		4-CN-Bn[d]	H	1.4 ± 0.1	34 ± 1	>40	40	>40	>40
2o		4-OCH_3-Bn[d]	H	10 ± 0.5	>40	>40	>40	>40	>40
2p		4-OH-Bn[d]	H	0.9 ± 0.05	>40	>40	>40	20 ± 0.1	>40
2q		$CH_2(C{=}O)N(CH_3)_2$	H	8.9 ± 0.2	40 ± 2	>40	>40	>40	>40
2r		$CH_2(C{=}O)$Morph[e]	H	24 ± 2	40 ± 2	>40	>40	>40	>40
3a	2-F	H	Et	20 ± 2	27	>40	>40	15 ± 2	>40
3b	4-F	H	Et	4.1 ± 0.2	>40	11	>40	6.3 ± 0.1	>40
3c	3-F	H	Et	6 ± 0.5	44 ± 4	>40	>40	30 ± 2	>40
3d	4-CN	H	Et	4.7 ± 0.2	>40	>40	>40	30 ± 2	>40
3e	H	Bn[d]	Et	>40	>40	>40	>40	nt	nt
3f	H	4-F-Bn[d]	Et	>40	>40	>40	>40	nt	nt
3g	H	4-CN-Bn[d]	Et	>40	>40	>40	>40	nt	nt
4a	2-F	H	H	1.7 ± 0.2	27 ± 0.5	>40	>40	20 ± 0.8	>40
4b	4-F	H	H	0.58 ± 0.03	40 ± 1	>40	>40	>40	>40
4c	3-F	H	H	0.78 ± 0.04	35 ± 1	>40	>40	>40	>40
4d	4-CN	H	H	1.1 ± 0.02	40 ± 2	>40	>40	>40	>40
4e	H	Bn[d]	H	16 ± 0.5	20 ± 1	>40	>40	>40	>40
4f	H	4-F-Bn[d]	H	9.5 ± 0.1	>40	>40	40	9 ± 0.12	>40
4g	H	4-CN-Bn[d]	H	6.8 ± 0.2	>40	>40	40	40 ± 3.3	>40

[a]Inhibitory concentration 50% (μM) determined from dose−response curves. [b]Effective concentration 50% (μM). [c]Ph: phenyl. [d]Bn: benzyl. [e]Morph: morpholine. [f]>40, no activity detected up to 40 μM tested concentration. [g]nt: not tested.

dx.doi.org/10.1021/jm4010187 | J. Med. Chem. 2013, 56, 7431−7441

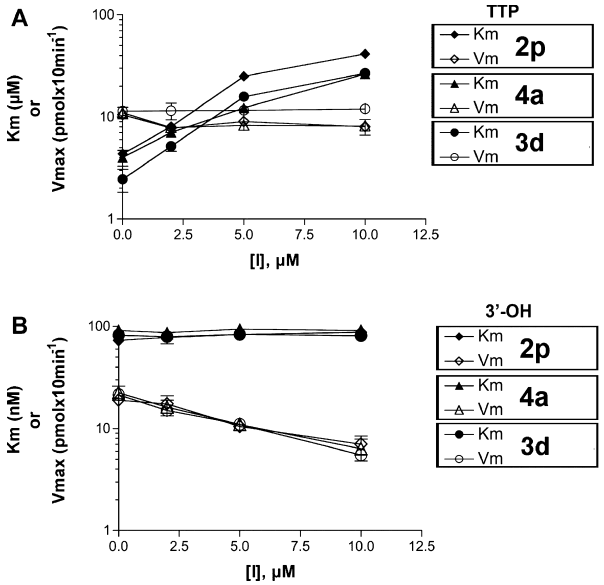

Figure 2. The diketohexenoic acid derivatives behave as nucleotide-competitive inhibitors. (A) Variation of the K_m (solid symbols) or V_{max} (open symbols) of TdT for the nucleotide substrate TTP as a function of increasing inhibitor concentrations. (B) Variation of the K_m (solid symbols) or V_{max} (open symbols) of TdT for the nucleic acid substrate (expressed as 3′-OH primer concentration) as a function of increasing inhibitor concentrations.

Table 2. Inhibitory Potencies and Mechanism of Inhibition of Nc Inhibitors against Human TdT of Compounds 2p, 3d, and 4a

	substrate TTP		substrate 3′-OH	
compd	K_i (μM)	mechanism[a]	K_i (μM)	mechanism[b]
2p	0.45 ± 0.1	C	0.5 ± 0.1	NC
3d	1.5 ± 0.2	C	1.7 ± 0.2	NC
4a	0.5 ± 0.1	C	0.4 ± 0.1	NC

[a]C: competitive. [b]NC: noncompetitive.

decreased expression of cyclin A compared to the control cells, indicating that cell cycle progression of cells into the S phase was markedly delayed and cells did not progress into G2 phase (Figure 3 B).

Subsequently, we examined p53 expression and caspase 3 cleavage as key regulators of cell cycle arrest and cell apoptotic death. Treatment of MOLT-4 cells with concentrations of compounds **3d** and **4f** corresponding to their respective IC_{50} values produced an increase of p53 levels after 30 h (Figure 3 C). Moreover, both **3d** and **4f** induced cleavage of caspase 3 only in MOLT-4 cells but not in HeLa cells, thus indicating a proapoptotic effect of these compounds (Figure 3 D).

Overall, these data correlate well with in vitro selectivity of compounds **3d** and **4f** for TdT.

Crystallization of TdT in Complex with Nc Inhibitors. To precisely identify the binding site of the Nc inhibitors described above, cocrystals of TdT with compounds **4b** and **4c** were grown and the structures solved at 2.4 and 2.6 Å resolution, respectively. Table S2 (see Supporting Information) summarizes the results of data collection and refinement statistics.

Both compounds **4b** (F in para) and **4c** (F in meta) nicely fit in the final $2F_o - F_c$ maps (Figure 4). The inhibitors are bound close to the deoxynucleotide triphosphate (dNTP) binding site.

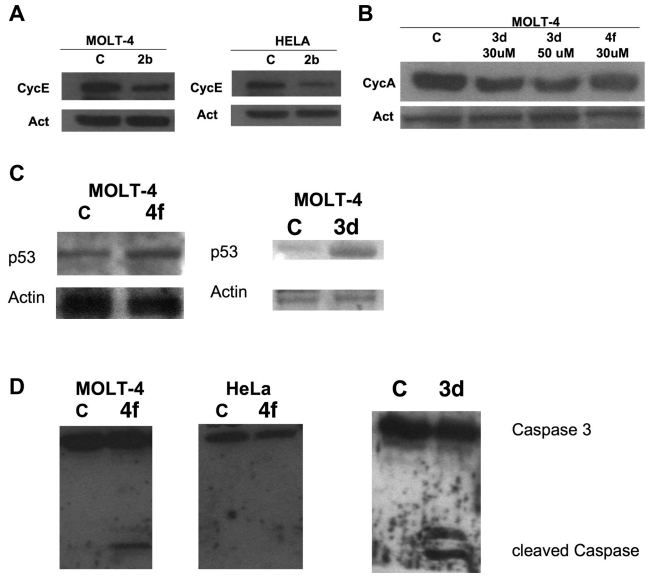

Figure 3. Western blot analysis: cyclin E expression in MOLT-4 and HeLa cells (A) treated with **2b** at 30 μM and (C) untreated; (B) cyclin A expression in MOLT-4 cells treated with different concentrations of **3d** (30 and 50 μM) and **4f** (30 μM) compared to control cells; (C) p53 levels in MOLT-4 cells treated with **4f** (9 μM) and **3d** (30 μM); (D) caspase 3 cleavage induced by **3d** and **4f** in MOLT-4 cells but not in HeLa cells.

The polar tails of **4b** and **4c** are located in the same place and point toward a polar cavity (Figure 4). They both interact via hydrogen bonds and electrostatic interactions with the COOH of the last amino acid of the TdT and with the NH_2 main chain atoms of Q455.

In addition the carboxy tail of **4b** binds the NH_2 backbone atom of R454, while the carbonyl group between the phenyl and the pyrrole rings of **4c** binds a water molecule. The main difference between the binding sites of two inhibitors is the localization of the aromatic heads. Whereas the phenyl ring of **4b** is nicely stacked against W450 (about 4 Å), the same moiety of **4c** is deeply buried below the active site: the fluorine contacts the NH_2 main chain atom of D345 (3.0 Å) and the peptide carbonyl of T331 (2.6 Å). The middle part of each inhibitor (from the alcohol to the carbonyl between the rings) does not interact with the protein (Figure S1 of Supporting Information). Both inhibitors can be seen as two anchoring moieties (aromatic head and polar tail) linked together. Each of these parts may have a low affinity for the TdT, but when they are linked together, the binding energies add up and the affinity constants are multiplied.

Analysis of the *B* factors of the inhibitors shows that they are slightly higher than the ones of the protein with a mean deviation compared to the mean protein *B* factors of 1.5σ and 1.3σ for **4b** and **4c**, respectively.

Cocrystals of Tdt with the Single-Stranded DNA Primer and the Inhibitors. It is possible to cocrystallize Tdt with both a primer strand and an inhibitor. Two data sets were collected at 2.9 and 2.6 Å for **4c** and **4b**, respectively. These data confirm that the inhibitors occupy the dNTP binding site in exactly the same place as previously observed. There is clear electron density for the phosphate backbone of the primer strand, but not much for the bases (Figure S2 in Supporting Information). In addition the base at the 3′-end could not be modeled in the structure. These features are

dx.doi.org/10.1021/jm4010187 | J. Med. Chem. 2013, 56, 7431−7441

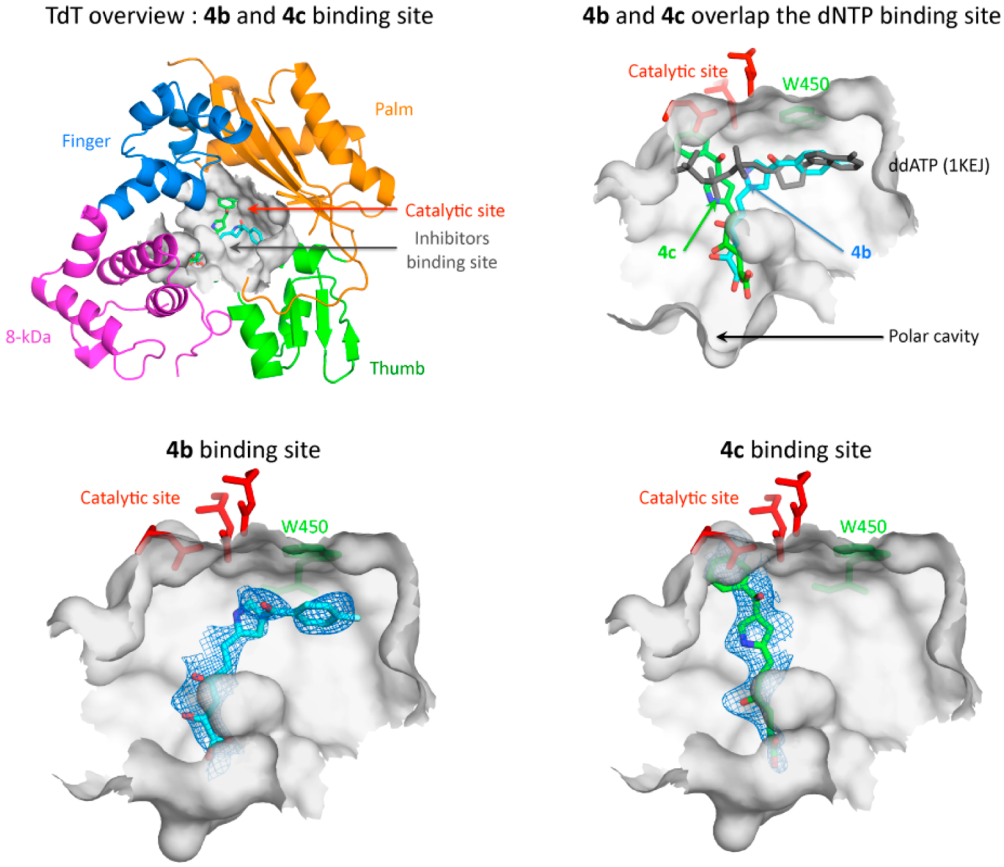

Figure 4. Overview of the TdT and omit maps. The upper left panel depicts the overall structure of TdT and the Nc binding site. The catalytic site is colored in red, whereas the inhibitor binding site is represented as a gray surface. The upper right panel shows a superposition of ddATP (PDB code 1KEJ) binding site, **4b**, and **4c**. The inhibitors impair the stable binding of the nucleotide. The lower panels show the final density maps with each of the inhibitors bound to the TdT. The two tails of the inhibitors are located at the same place, but the apolar head points toward different localizations. The $2F_o - F_c$ maps have been contoured at 1.0σ (dark blue).

also observed in the complexs of TdT, ssDNA, and dATP analogues.

Comparison of These Binary Complexes and the Binary Complex of TdT with an Incoming ddATP. From superimposition of the binary complex TdT with ddATP[18] (PDB code 1KEJ), the structures with **4b** and **4c** show a clear overlap of the inhibitor binding site and the nucleotide binding site (Figure 4). The phenyl ring of **4b** occupies the same place as the aromatic ring of the base of the incoming nucleotide. The phenyl ring of **4c** overlaps the phosphate β of the ddATP and the metal B. These superimpositions highlight the two roles of the aromatic head: (i) preventing the binding of the natural substrates (dNTPs) and (ii) anchoring the molecule within the polymerase through its polar tail.

DISCUSSION

In this work, we described the first non-nucleoside selective inhibitors of human TdT and showed that they have a common mode of action, namely, competing with the binding of the nucleotide substrate. They represent a novel class of Nc inhibitors.

The structures of the complexes between the Nc inhibitors **4b** and **4c** and TdT presented here indicate that these compounds indeed physically interfere with the binding of the incoming nucleotide. Both are bound near the active site of TdT. The polar tails of **4c** and **4b** are located in a similar place and point toward a polar cavity. The aromatic part of **4c** is deeply buried under two of the catalytic aspartates residues, whereas the phenyl ring of **4b** is stacked against W450. The difference between the two binding modes is certainly due to the different substituents of the phenyl ring: in particular, the fluorine atom in para would not fit in the cavity below the catalytic site so that it is understandable that it finds another binding pocket. The specific interaction between the fluorine atom of **4c** with the peptide NH_2 group of D345 and the peptide carbonyl group of T331 favors the binding of the inhibitor near the three conserved aspartates of the active site. It is remarkable that the different localization of the aromatic rings of **4b** and **4c** allows us to propose a binding mode for **4e**, without any further hypothesis. This is shown in Figure 5, where the polar tail of the three inhibitors were superimposed. The resulting model shows that if the first phenyl group is stacked against W450 as in **4b**, the second phenyl that is linked to the pyrrole nitrogen atom will point below the active site exactly as in **4c**.

Both inhibitors overlap with the binding site of the incoming nucleotide; therefore, they physically compete with the dNTP. This conclusion is consistent with the competitive binding mode with respect to dNTP observed in the in vitro experiments. On the other hand their binding mode in the TdT is compatible with the simultaneous binding of the ssDNA in a competent complex, which is consistent with their noncompetitive binding mode with respect to the DNA (see Figure S2). In addition, these structures are also consistent with the kinetic

dx.doi.org/10.1021/jm4010187 | J. Med. Chem. 2013, 56, 7431−7441

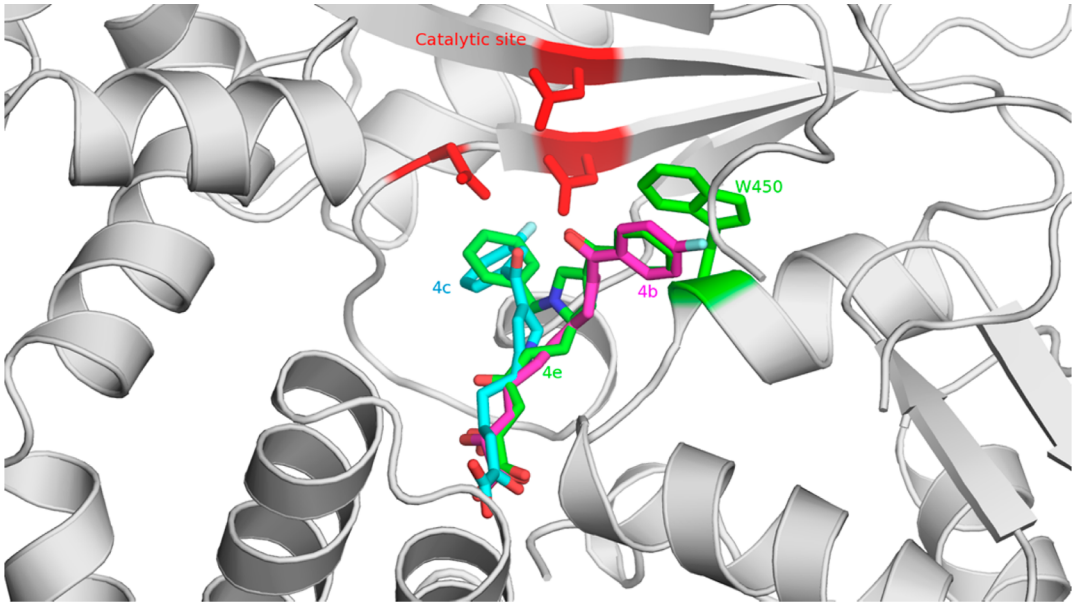

Figure 5. Model of the binding of TdT with compound **4e** based on the structures of compounds **4b** and **4c** and superimposition of their carboxy-terminal part.

data, showing that the Nc compounds have higher dissociation rates from the TdT when both the nucleotide and the DNA are present in the active site, while they have similar if not slower dissociation rates when only DNA is present, with respect to the free enzyme.

The identification of the interactions of the Nc inhibitors to TdT opens the possibility of rationally designing more potent compounds. In particular, new inhibitors can be designed based on the postulated structure (Figure 5) of **4e**, where the two phenyl rings are arranged to occupy the positions observed in **4b** and **4c.** These positions allow a fragment-based approach for designing better drugs.

Indeed the phenyl that points below the active site could easily be changed into a more polar group. For instance, one can think of replacing it by a phenol side chain or a guanidinium group to bind directly the catalytic aspartates. Straightforward modeling indicates there is room for this. A second approach for this group would be to bind the catalytic metals instead of the aspartates. Two such metals can be found in all DNA polymerases. The metal A activates the 3′-OH in order to attack the phosphodiester bond of the incoming dNTP. Metal B helps to bind the dNTP in the active site.[21] Substituting the second phenyl ring of **4e** into a histidine side chain would contribute to building a very strong binding site for a Zn^{2+} in the metal A site. This modification should increase both the affinity and the solubility of inhibitors while better competing with the binding of the incoming nucleotide.

For the other phenyl group, we note that making use of a stacking interaction with W450 is only possible for Tdt and pol μ (and not for pol β or pol λ where W450 is replaced by an F and flanked by a neighboring Y residue). The binding of inhibitors specific to TdT instead of other pol X may also be enhanced using the scaffold of **4b**. Close to the fluorine atom in para, an asparagine N474 is present in TdT (Y in pol β and pol λ, S in pol μ). If this fluorine atom is replaced by an amide group or a hydroxyl group, a hydrogen bond would anchor tighter the inhibitor to its binding site while conferring a better specificity because in pol μ it would face a serine instead of an asparagine; therefore, the corresponding hydrogen bond would be weaker.

There was a clear correlation between selective inhibition of TdT by the Nc compounds reported here and selective toxicity toward TdT^+ cells, such as MOLT-4, with respect to HeLa cells that do not express TdT. The cytotoxic effect in MOLT-4 cells was due to apoptosis. Recently described non-natural nucleoside inhibitors of TdT[22] were also able to induce cell death through apoptosis in MOLT-4 cells, underlying a common mechanism of action. We observed a strong block of the cell cycle in G1 in MOLT-4 cells treated with our compounds. The relationships between TdT and cell cycle progression on cancer cells are poorly understood; however, TdT has been shown to participate in a highly mutagenic NHEJ pathway for DNA DSBs repair.[23] DSBs are the most lethal form of DNA damage for the cell. They are repaired by homologous recombination during S-phase and by NHEJ in G1/G2. A gradient of template dependency and fidelity has been shown in reconstituted NHEJ in vitro systems among the different DNA polymerase involved: pol λ, pol μ, and TdT, with the last being responsible for highly mutagenic end-joining.[23] High TdT levels in cancer cells might compete with the other enzymes during NHEJ, rendering these cells highly resistant to DSB inducing agents but also more prone to mutations, because of the low fidelity of the end joining reaction. The strong block in G1 and the apoptosis observed upon inhibition of TdT by our Nc compounds are consistent with the phenotype observed upon induction of DSB accumulation in cells and suggest that MOLT-4 cells may accumulate high levels of endogenous DSBs, likely as a result of their high proliferative rate, and are heavily dependent on TdT for their repair.

Inhibition of NHEJ has also been shown to enhance sensitization of cancer cells to interstrand-cross-link inducing agents such as chlorambucil, commonly used in the treatment of leukemia.[24] Thus, our Nc compounds hold the potential to be used in combination therapies with other anticancer drugs.

dx.doi.org/10.1021/jm4010187 | J. Med. Chem. 2013, 56, 7431−7441

EXPERIMENTAL SECTION

Chemistry. General Procedures. Melting points were determined with a Büchi 530 capillary apparatus and are uncorrected. The purity of compounds was always >95%, determined by high pressure liquid chromatography (HPLC). HPLC analyses were carried out with a Shimadzu LC-10AD VP CTO-10AC VP instrument. The column used was generally Discovery Bio Wide Pore C18 (10 cm × 4.6 mm, 3 μm). Infrared (IR) spectra were recorded on a Perkin-Elmer Spectrum-One spectrophotometer. ^{1}H NMR spectra were recorded on a Bruker AC 400 spectrometer. Büchi Syncore was used for parallel synthesis using 50 mL test tubes. The reaction solutions were purified on using SPE and filtration column (charged with silica gel pad) in a Biotage FlashVac-10 system. Merk silica gel 60 F_{254} plates were used for analytical TLC. Developed plates were visualized by UV light. Column chromatographies were performed on silica gel (Merck, 70−230 mesh) or alumina (Merck, 70−230 mesh). Concentration of solution after reactions and extractions involved the use of a rotary evaporator operating at reduced pressure of approximately 20 Torr. The purity of newly synthesized compounds has been evaluated by elemental analysis. Analytical results agreed to within ±0.40% of the theoretical values (see Supporting Information), confirming the ≥95% purity. Dimethylsulfoxide-d_6 99.9% (code 44,139-2) and deuterochloroform 98.8% (code 41,675-4) of isotopic purity (Aldrich) were used. Solvents were reagent grade and, when necessary, were purified and dried by standard methods. Organic solutions were dried over anhydrous sodium sulfate (Merck).

Microwave Irradiation Experiments. Microwave reactions were conducted using a CEM Discover system unit (CEM. Corp.; Matthews, NC). The machine consists of a continuous focused microwave-power delivery system with operator selectable power output from 0 to 300 W. The temperature of the contents of the vessel was monitored using a calibrated infrared temperature control mounted under the reaction vessel. All experiments were performed using a stirring option whereby the contents of the vessel are stirred by means of a rotating magnetic plate located below the floor of the microwave cavity and a Teflon-coated magnetic stir bar in the vessel.

Syntheses. General procedures are reported.

General Procedure for *N*-Alkylindole-3-carboxaldehydes 5a−g,k−o,q. Thirteen tubes were charged with a solution of indole-3-carboxaldehyde (1.34 g, 9.2 mmol) in 20 mL of dry DMF treated with NaH (0.58 g, 14.7 mmol) and were placed in the Büchi Syncore reactor. After development of H_2, the solution was treated with the appropriate halide (11 mmol) and the resulting mixture was stirred with bascular stirring in a Büchi Syncore at room temperature at 250 rpm for 1 h.

For **5b−g**, the solutions were diluted with water and extracted with ethyl acetate. The organic layers were washed with brine, dried over anhydrous Na_2SO_4, filtered, and evaporated in vacuum to obtain derivatives **5b−g** as oil.

For **5a,k−o**, the solutions were diluted with water and the solid that formed was filtered using a FlashVac-10 system. The solid was washed with water and light petroleum ether to give derivatives **5a,k−o** as solid.

For **5q**, the residue was dissolved in ethyl acetate, washed with 1 N HCl (3 times) and brine (three times), and dried, and the solvent was evaporated under reduced pressure. The crude product was chromatographed with flash chromatography on silica gel (ethyl acetate/*n*-hexane mixture, 1:5, as eluent) to furnish 4.05 g (56.6%) of pure **5q** as a white solid.

1-(4-Hydroxybenzyl)-1*H*-indole-3-carboxaldehyde (5p). A solution of **5o** (6 g, 22.6 mmol) in 246 mL of CH_2Cl_2 was added dropwise to a solution of 1 M BBr_3 in CH_2Cl_2 (6.3 mmol, 119.25 mL) cooled at −45 °C under argon stream. The mixture was stirred at −45 °C for 1 h and then was treated with water. After placement of the mixture at room temperature, the formed precipitate was collected by filtration. The solid was washed with water and light petroleum ether to give 5 g (76%) of pure **5p** as a red solid.

General Procedure for 1-(4-Phenyl)-1*H*-indole-3-carboxaldehydes 5h−j. Indole-3-carboxaldehyde (48 mmol), cupric acetate (12 mmol), the appropriate arylboronic acid (8.4 mmol), and 1:1 NMP/pyridine mixture (5 mL) were placed in a 100 mL round-bottom flask. The bottom part of the flask was placed into the microwave cavity (60 W, 120 °C, 50 s, open vessel). The microwave irradiation was repeated six times, and after each cycle, the mixture was cooled and cupric acetate (12 mmol), phenylboronic acid (84 mmol), and NMP/pyridine mixture (5 mL) was added. After cooling, the mixture was diluted with tetrahydrofuran and filtered off and the solvent was evaporated. The residue was dissolved in ethyl acetate, washed with 1 N HCl (20 times) and brine (three times), and dried, and the solvent was evaporated under reduced pressure. The crude product was purified by column chromatography to furnish the derivatives **5h−j**.

2-(3-Formyl-1*H*-indol-1-yl)acetic Acid (5r). Compound **5q** (3.95 g, 15.2 mmol) was treated with dichloromethane/trifluoroacetic acid mixture 1:1 (305 mL) to obtain a solution at 0.05 M. The mixture was stirred for 16 h at room temperature. After removal of the solvent, the residue was triturated with diethyl ether for 1 h. The solid was filtered and washed with diethyl ether to obtain 2.8 g of pure **5r** as a pink solid (92%).

General Procedure for 3-Formyl-1*H*-indoles 5s,t. **5r** (2.6 mmol) is solubilized in 13 mL of dry DMF to obtain a 0.2 M solution. The solution was treated with base (2.6 mmol) and HBTU (2.6 mmol). The solution was cooled at 0 °C and treated with DIEA (7.8 mmol). After the addition, the mixture was stirred for 2 days at room temperature. Ethyl acetate was added to the mixture, and the obtained mixture was washed with 1 N HCl (three times), $NaHCO_3$ ss (three times), and brine (three times) and dried, and the solvent was evaporated under reduced pressure to obtain derivatives **5s,t**.

General Procedure for Pyrroles 7a−e. To a solution of DMF (81.9 mmol) in 1,2-dichloromethane (18 mL) cooled in an ice bath was added dropwise a solution of oxalyl chloride (81.9 mmol) in 1,2-dichloroethane (12 mL) in 20 min. After the addition, the formed suspension was stirred at room temperature for 15 min. The suspension was placed again in an ice bath, and then to it was added a solution of pyrrole (74.5 mmol) in dichloroethane (15 mL) dropwise in 20 min. The reaction mixture was stirred at room temperature for 15 min and was treated with $AlCl_3$ (163.9 mmol) with care and then with the appropriate benzoyl chloride (74.5 mmol). The reaction mixture was stirred at room temperature for 3 h 40 min, treated with crushed ice and water (745 mL) and a solution of 50% NaOH (60 mL), and stirred for 10 min. The aqueous phase was acidified with concentrated HCl until pH 4 was reached. The formed precipitate was collected by filtration and washed with water and light petroleum ether to obtain pure derivatives **7a−e**.

General Procedure for Pyrroles 8a−c. Three tubes were charged with a mixture of pyrrole **7e** (7.5 mmol) and the appropriate benzyl bromide (8.3 mmol) in diethyl ether (37.5 mL) and chloroform (57 mL) and placed in the Büchi Syncore reactor. The mixtures were treated with tetrabutylammonium bromide (0.75 mmol) and crushed NaOH (18.8 mmol). The reaction mixtures were stirred with bascular stirring in Büchi Syncore at room temperature at 250 rpm for 3 h, then treated with 1.2 mL of water and stirred at room temperature for a further 2 h. The formed precipitates were filtered off on a silica gel pad and washed with chloroform using a FlashVac-10 system. The filtrates were dried and evaporated under reduced pressure, obtaining **8a−c**.

General Procedure for 4-(Indol-3-yl)but-3-en-2-ones 6a−r. Eighteen tubes were charged with a solution of appropriate aldehyde **5a−p,s,t** (31.1 mmol) in 105.7 mL of acetone and placed in the Büchi Syncore reactor. The solutions were treated with 45.2 mL of 5 N NaOH and stirred with bascular stirring in Büchi Syncore at 50 °C at 250 rpm for 2 nights and then were treated with water. The mixtures were extracted with ethyl acetate. The collected organic extracts were washed with brine (three times) and dried, and the solvent was evaporated under reduced pressure to obtain pure derivatives **6a−r**.

General Procedure for Pyrroles 9a−g. Eight tubes were charged with a solution of appropriate aldehyde **7a−d** or **8a−c** (41.2 mmol) in 32.84 mL of acetone and placed in the Büchi Syncore reactor. The solutions were treated with barium hydroxide (4.12 mmol) and stirred with bascular stirring in Büchi Syncore at 50 °C at 250 rpm for 5 h. After cooling, the mixtures were treated with water and acidified

dx.doi.org/10.1021/jm4010187 | *J. Med. Chem.* 2013, 56, 7431−7441

with 1 N HCl until pH 5 was reached. The mixtures were extracted with ethyl acetate. The collected organic extracts were washed with brine (three times), dried, and the solvent was evaporated under reduced pressure to obtain pure derivatives **9a−g**.

General Procedure for Diketo Esters 1a−r and 3a−g. The appropriate acetyl derivative **6a−r** or **9a−g** (31 mmol) and diethyl oxalate (62 mol) were dissolved in 31 mL of dry THF and treated, under argon stream, with NaOEt obtained by the dissolution of Na (63 mmol) in 56 mL of absolute ethanol. The mixture was stirred at room temperature for 1 h 30 min, then was pured into *n*-hexane (704 mL). The collected precipitate was vigorously stirred for 30 min in 1 N HCl (704 mL). The solid that formed was filtered, washed with water and light petroleum ether, and dried under IR lamp to afford the pure diketo esters **1a−r** and **3a−g**.

General Procedure for Diketo Acids 2a−r and 4a−g. A mixture of 1 N NaOH (9.5 mL) and the appropriate ester **1a−r** or **3a−g** (1.9 mmol) in 1:1 THF−methanol (9.3 mL) was stirred at room temperature for 30 min and then poured into crushed ice. The mixture was treated with 1 N HCl until pH 3 was reached and extracted with ethyl acetate (three times). The collected organic extract was washed with brine (three times) and dried, and the solvent was evaporated under reduced pressure to give the pure diketo acids **2a−r** and **4a−g**.

Details concerning characterization data are reported in the Supporting Information for compounds **1a−r**, **2a−r**, **3a−g**, **4a−g**, **5a−t**, **6a−r**, **7a−e**, **8a−c**, **9a−g**.

Biological Assay. Enzymes and Proteins. Recombinant full length human DNA polymerase λ was generated and purified as described.[25] After purification, the protein was >90% homogeneous, as judged by sodium dodecyl sulfate (SDS)−polyacrylamide gel electrophoresis (PAGE) and Coomassie staining. Recombinant DNA polymerase β and TdT were from Trevigen.

DNA Polymerase Assay. Human DNA polymerase λ activity on poly(dA)/oligo(dT)$_{10:1}$ was assayed in a final volume of 25 μL containing 50 mM Tris-HCl (pH 7.0), 0.25 mg/mL BSA, 1 mM DTT, 0.5 mM $MnCl_2$, 0.2 μM poly(dA)/oligo(dT)$_{10:1}$ (3′-OH ends), 50 nM DNA polymerase λ, and 5 μM [^{3}H]-2′-deoxythymidine 5′-triphosphate (dTTP) (5 Ci/mmol), unless otherwise indicated in the figure captions. All reactions were incubated for 15 min at 37 °C unless otherwise stated, and the DNA precipitated with 10% trichloroacetic acid. Insoluble radioactive material was determined by scintillation counting as described. DNA polymerase β activity was assayed as described.[25]

Terminal Deoxyribonucleotidyl Transferase Assay. DNA polymerase λ and TdT terminal transferase activities were assayed in a final volume of 25 μL containing 50 mM Tris-HCl (pH 7.0), 0.25 mg/mL BSA, 1 mM DTT, 0.5 mM $MnCl_2$, 0.2 μM ss 27-mer DNA oligonucleotide, unless otherwise stated. Enzymes and [^{3}H]dNTPs (10 Ci/mmol) were added as indicated in the figure captions. All mixtures were incubated at 37 °C for 10 min, unless otherwise indicated in the figures, and the DNA precipitated with 10% trichloroacetic acid. Insoluble radioactive material was determined by scintillation counting as described.[26]

Inhibition Assays. Reactions were performed under the conditions described for the terminal deoxyribonucleotidyl transferase activity assay. Incorporation of radioactive dTTP into the ss 27-mer oligodeoxynucleotide at different concentrations of DNA or dNTP was monitored in the presence of increasing amounts of inhibitor as indicated in the figure captions. Dose−response curves were generated by computer fitting of the data to the relationship $E_{(\%)} = E_{max}/(1 + I/ID_{50})$ where $E_{(\%)}$ is the fraction of enzyme's activity measured in the presence of the inhibitor, E_{max} is the activity in the absence of the inhibitor, I is the inhibitor concentration, and ID_{50} is the inhibitor concentration at which $E_{(\%)} = 0.5E_{max}$. The ID_{50} values at different substrate concentrations where used to determine the K_i, according to the Cheng−Prusoff relationship for a fully competitive model, in the form $ID_{50} = K_i(1 + S/K_m)$ where S is the concentration and K_m is the apparent affinity of the competing substrate.

Cell-Based Assay. The TDT$^+$ cell line MOLT-4 (a human early T cell leukemia cell line) and the TDT-cell line HeLa were used. The TdT status of MOLT-4 cells has been described by McCaffrey and colleagues.[14,27] Human lymphoblastic leukemia MOLT-4 (TdT-positive) and cervical adenocarcinoma HeLa (TdT-negative) cell lines were grown at 37 °C in RPMI-1640 and Dulbecco's modified Eagle medium, respectively, both containing 10 mM glucose supplemented with 10% fetal calf serum and 100 units/mL each of penicillin and streptomycin and 2 mmol/L glutamine. For each experiment, cells were placed in fresh medium, cultured in the presence of synthesized compounds (from 0.1 to 100 mm), and followed for further analyses.

Cell viability was determined using the 3-[4,5-dimethylthiazol-2,5-diphenyl-2*H*-tetrazolium bromide (MTT) colorimetric assay. The test is based on the ability of mitochondrial dehydrogenase to convert, in viable cells, the yellow MTT reagent (Sigma Chemical Co.; St. Louis, MO) into a soluble blue formazan dye. Cells were seeded into 96-well plates to a density of 10^5 cells/100 μL well. After 24 h of growth to allow attachment of adherent cells to the wells, compounds were added at various concentrations (from 0.1 to 100 mM). After 24 or 48 h of growth and after removal of the culture medium, 100 μL/well of medium containing 1 mg/mL of MTT was added. Cell cultures were further incubated at 37 °C for 2 h in the dark. The solution was then gently aspirated from each well, and the formazan crystals within the cells were dissolved with 100 μL of dimethylsulfoxide (DMSO). Optical densities were read at 550 nm using a Multiskan Spectrum Thermo Electron Corporation reader. Results were expressed as percentage relative to vehicle-treated control (0.5% DMSO was added to untreated cells). IC_{50} (concentration eliciting 50% inhibition) values were determined by linear and polynomial regression. Experiments were performed in triplicate.

Molt-4 and HeLa cells (2.5×10^5 cells/mL) in 12-well tissue culture plates were incubated for 24 h in the presence or absence (vehicle-treated cells) of **3e**, **2b**, and **4g** compounds. Cells were then washed with phosphate buffered saline (PBS) 1× and suspended by trypsinization. Cells were centrifuged at 2000 rpm for 5 min, then washed with PBS 1× and resuspended in fresh medium. Finally, cells were incubated in the dark with a staining solution containing 0.1% sodium citrate, 0.1% Triton X-100, and 50 mg/mL propidium iodide at 4 °C for 30 min. Samples were analyzed by Necton Dickinson FACScan flow cytometer. Cell cycle distribution, expressed as percentage of cells in the G0/G1, S, and G2/M phases, was calculated using ModFit LT 3.0 software. Apoptotic cells are expressed as percentage of hypodiploid nuclei.

Cells were plated in flasks (1×10^6 cells) in normal culture conditions and incubated with or without **3e**, **2b**, and **4g** compounds. At the indicated times, cells were lysed using an ice cold lysis buffer (50 mM Tris, 150 mM NaCl, 10 mM ethylenediaminetetraacetic acid (EDTA), 1% Triton) supplemented with a mixture of protease inhibitors containing antipain, bestatin, chymostatin, leupeptin, pepstatin, phosphoramidon, Pefabloc, EDTA, and aprotinin (Boehringer, Mannheim, Germany). Equivalent amounts of protein were loaded on 8−12% sodium dodecyl sulfate (SDS)−polyacrylamide gels and electrophoresed followed by blotting onto nitrocellulose membranes (Bio-Rad, Germany). After blotting with 5% (w/v) fat-free milk powder and 0.1% Tween 20 in TBS, the membrane was incubated overnight at 4 °C with specific antibodies against cyclin E2, cyclin A, p53, and caspase 3 at the concentrations indicated by the manufacter's protocol (Santa Cruz Biotechnology). The antibody was diluted in Tris-buffered saline/Tween 20 5% milk powder. Following incubation with horseradish peroxidase-conjugated secondary antibodies, bands were detected by enhanced chemiluminescence (ECL kit, Amersham, Germany). Each filter was then probed with rabbit polyclonal anti-actin (Santa Cruz Biotechnology). Level of expression of detected bands was quantified by NIH ImageJ 1.40 after normalization with actin.

Details concerning the biological results are reported in the Supporting Information for **1a−r**, **2a−r**, **3a−g**, and **4a−g**.

Structural Study. Crystallization and Data Collection. TdT (10 mg/mL) was incubated with inhibitors (1 mM final) for 30 min at 4 °C prior to setting up crystallization drops. All crystals were grown overnight at room temperature. Complexes with **4c** were grown in Greiner plates in a solution containing 22% polyethylene glycol (PEG)

4000, 200 mM ammonium formate, and 100 mM 2-(*N*-morpholino)-ethanesulfonic acid (MES), pH 6.5. Complexes with **4b** were grown in a solution containing 20% PEG 4000, 200 mM sodium formate, 100 mM MES, pH 6.0. Complexes of the TdT with the inhibitors and DNA (5′-GCCG-3′, purchased from Eurogentec, Seraing, Belgium) were grown by incubating a mixture of the protein, the primer strand (ratio 1:1.2), and the inhibitor in the same conditions as described earlier. Note that the wild-type protein has been used with **4c**, whereas a mutant of loop1 (L398A) was crystallized with **4b**. Crystals were cryoprotected using a solution supplemented with 30% glycerol prior to flash-freezing at 100 K. Data have been integrated with XDS,[28] processed with POINTLESS,[29] scaled, and merged with SCALA[30] (CCP4). The molecular replacement was achieved with PHASER[31] using 1JMS[18] as a search model. The refinement has been carried out by BUSTER-TNT[32] using automatic water updating and TLS defined with TLSMD server.[33] Manual building of the model was achieved with COOT.[34] For each ligand a PDB file was created with the PRODRG[35] server, and subsequent restraints for BUSTER-TNT[32] and COOT were calculated with PDB2TNT. The quality of the final models was checked with MolProbity.[36]

■ ASSOCIATED CONTENT

Ⓢ Supporting Information

Details concerning the chromatographic system used, yields (%), melting points (°C), recrystallization solvents, IR, ^{1}H NMR, and elemental analysis results, and biological assays for all new compounds and also crystals structures of the complex with single-stranded DNA. This material is available free of charge via the Internet at http://pubs.acs.org.

Accession Codes

All structures including structure factors have been deposited in the Protein Data Bank under the accession codes 4IQT, 4IQU, 4IQV, and 4IQW. See also Table S2 in the Supporting Information for a summary of some crystallographic information.

■ AUTHOR INFORMATION

Corresponding Author

*Phone: +39-06-4969-3247. E-mail: roberta.costi@uniroma1.it.

Author Contributions

[#]G.M. and R.D.S. share the senior authorship.

The manuscript was written through contributions of all authors. All authors have given approval to the final version of the manuscript.

Notes

The authors declare no competing financial interest.

■ ACKNOWLEDGMENTS

This work has been partially supported by an Italian Cancer Research Association AIRC IG Grant 12084 to G.M., "Sapienza" Ateneo Funds to R.D.S, and ARC Grant 3155 to J.G. and M.D.

■ ABBREVIATIONS USED

TdT, terminal deoxynucleotidyl transferase; DSB, double strand break; NHEJ, nonhomologous end joining; dNTP, deoxynucleotide triphosphate; ALL, acute lymphocytic leukemia; AML, acute myelocitic leukemia; K_m, affinity constant; V_{max}, maximal velocity; Nc, nucleotide-competitive; K_i, inhibitory constant; E, free enzyme; E:DNA, binary enzyme−nucleic acid complex; E:DNA:dNTP, ternary enzyme−nucleic acid−nucleotide; k_{on}, apparent rate of association; k_{off}, apparent rate of dissociation; HPLC, high pressure liquid chromatography; IR, infrared; SDS, sodium dodecyl sulfate; PAGE, polyacrylamide gel electrophoresis; dTTP, 2′-deoxythymidine 5′-triphosphate; MTT, 3-[4,5-dimethylthiazol-2,5-diphenyl-2*H*-tetrazolium bromide; DMSO, dimethylsulfoxide; PBS, phosphate buffered saline; EDTA, ethylenediaminetetraacetic acid; PEG, polyethylene glycol; MES, 2-(*N*-morpholino)-ethanesulfonic acid

■ REFERENCES

(1) Alberts, B. DNA replication and recombination. *Nature* **2003**, *421*, 431−435.

(2) Bollum, F. J. Thermal conversion of nonpriming deoxyribonucleic acid to primer. *J. Biol. Chem.* **1959**, *234* (10), 2733−2734.

(3) Bollum, F. J. Chemically defined templates and initiators for deoxypolynucleotide synthesis. *Science* **1964**, *144*, 560.

(4) Bollum, F. J. Calf thymus polymerase. *J. Biol. Chem.* **1960**, *235*, 2399−2403.

(5) Krayevsky, A. A.; Victorova, L. S.; Arzumanov, A. A.; Jasko, M. V. Terminal deoxynucleotidyl transferase: catalysis of DNA (oligodeoxynucleotide) phosphorylation. *Pharmacol. Ther.* **2000**, *85* (3), 165−173.

(6) Benedict, C. L.; Gilfillan, S.; Thai, T. H.; Kearney, J. F. Terminal deoxynucleotidyl transferase and repertoire development. *Immunol. Rev.* **2000**, *175*, 150−157.

(7) Baltimore, D. Is terminal deoxynucleotidyl transferase a somatic mutagen in lymphocytes? *Nature* **1974**, *248*, 409−411.

(8) Desiderio, S. V.; Yancopoulos, G. D.; Paskind, M.; Thomas, E.; Boss, M. A.; Landau, N.; Alt, F. W.; Baltimore, D. Insertion of N regions into heavy-chain genes is correlated with expression of terminal deoxytransferase in B cells. *Nature* **1984**, *311*, 752−755.

(9) Benedict, C. L.; Kearney, J. F. Increased junctional diversity in fetal B cells results in a loss of protective anti-phosphorylcholine antibodies in adult mice. *Immunity* **1999**, *10* (5), 607−617.

(10) Greaves, M.; Paxton, A.; Janossy, G.; Pain, C.; Johnson, S.; Lister, T. A. Acute lymphoblastic leukaemia associated antigen. III Alterations in expression during treatment and in relapse. *Leuk. Res.* **1980**, *4* (1), 1−14.

(11) Hoffbrand, A. V.; Ganeshaguru, K.; Janossy, G.; Greaves, M. F.; Catovsky, D.; Woodruff, R. K. Terminal deoxynucleotidyl-transferase levels and membrane phenotypes in diagnosis of acute leukaemia. *Lancet* **1977**, *310* (8037), 520−523.

(12) Kung, P. C.; Long, J. C.; McCaffrey, R. P.; Ratliff, R. L.; Harrison, T. A.; Baltimore, D. Terminal deoxynucleotidyl transferase in the diagnosis of leukemia and malignant lymphoma. *Am. J. Med.* **1978**, *64* (5), 788−794.

(13) Venditti, A.; Del Poeta, G.; Buccisano, F.; Tamburini, A.; Aronica, G.; Bruno, A.; Cox-Froncillo, M. C.; Maffei, L.; Simone, M. D.; Papa, G.; Amadori, S. Biological pattern of AML-M0 versus AML-M1: response. *Blood* **1997**, *89* (1), 345−346.

(14) McCaffrey, R.; Bell, R.; Lillquist, A.; Wright, G.; Baril, E.; Minowada, J. Selective killing of leukemia cells by inhibition of TdT. *Haematol. Blood Transfus.* **1983**, *28*, 24−27.

(15) Plunkett, W.; Gandhi, V. Purine and pyrimidine nucleoside analogs. *Cancer Chemother. Biol. Response Modif.* **2001**, *19*, 21−45.

(16) Zhou, Y.; Achanta, G.; Pelicano, H.; Gandhi, V.; Plunkett, W.; Huang, P. Action of (*E*)-2′-deoxy-2′-(fluoromethylene)cytidine on DNA metabolism: incorporation, excision, and cellular response. *Mol. Pharmacol.* **2002**, *61*, 222−229.

(17) Locatelli, G. A.; Di Santo, R.; Crespan, E.; Costi, R.; Roux, A.; Hübscher, U.; Shevelev, I.; Blanca, G.; Villani, G.; Spadari, S.; Maga, G. Diketo hexenoic acid derivatives are novel selective non-nucleoside inhibitors of mammalian terminal deoxynucleotidyl transferases, with potent cytotoxic effect against leukemic cells. *Mol. Pharmacol.* **2005**, *68* (2), 538−550.

(18) Delarue, M.; Boulé, J. B.; Lescar, J.; Expert-Bezançon, N.; Jourdan, N.; Sukumar, N.; Rougeon, F.; Papanicolaou, C. Crystal structures of a template-independent DNA polymerase: murine terminal deoxynucleotidyltransferase. *EMBO J.* **2002**, *21*, 427−439.

(19) Moon, A. F.; Garcia-Diaz, M.; Batra, V. K.; Beard, W. A.; Bebenek, K.; Kunkel, T. A.; Wilson, S. H.; Pedersen, L. C. The X family portrait: structural insights into biological functions of X family polymerases. *DNA Repair* **2007**, *6* (12), 1709−1725.
(20) Moon, A. F.; Garcia-Diaz, M.; Bebenek, K.; Davis, B. J.; Zhong, X.; Ramsden, D. A.; Kunkel, T. A.; Pedersen, L. C. Structural insight into the substrate specificity of DNA polymerase μ. *Nat. Struct. Mol. Biol.* **2007**, *14*, 45−53.
(21) Joyce, C. M.; Steitz, T. A. Function and structure relationships in DNA polymerases. *Annu. Rev. Biochem.* **1994**, *63*, 777−822.
(22) Motea, E. A.; Lee, I.; Berdis, A. J. A non-natural nucleoside with combined therapeutic and diagnostic activities against leukemia. *ACS Chem. Biol.* **2012**, *7* (6), 988−998.
(23) Nick McElhinny, S. A.; Havener, J. M.; Garcia-Diaz, M.; Juárez, R.; Bebenek, K.; Kee, B. L.; Blanco, L.; Kunkel, T. A.; Ramsden, D. A. A gradient of template dependence defines distinct biological roles for family X polymerases in nonhomologous end joining. *Mol. Cell* **2005**, *19* (3), 357−366.
(24) Amrein, L.; Davidson, D.; Shawi, M.; Petruccelli, L. A.; Miller, W. H., Jr.; Aloyz, R.; Panasci, L. Dual inhibition of the homologous recombinational repair and the nonhomologous end-joining repair pathways in chronic lymphocytic leukemia therapy. *Leuk. Res.* **2011**, *35* (8), 1080−1086.
(25) Blanca, G.; Shevelev, I.; Ramadan, K.; Villani, G.; Spadari, S.; Hübscher, U.; Maga, G. Human DNA polymerase λ diverged in evolution from DNA polymerase β toward specific Mn++ dependence: a kinetic and thermodynamic study. *Biochemistry* **2003**, *42*, 7467−7476.
(26) Hubscher, U.; Kornberg, A. The delta subunit of *Escherichia coli* DNA polymerase III holoenzyme is the dnaX gene product. *Proc. Natl. Acad. Sci. U.S.A.* **1979**, *76*, 6284−6288.
(27) Kodama, E. N.; McCaffrey, R. P.; Yusa, K.; Mitsuya, H. Antileukemic activity and mechanism of action of cordycepin against terminal deoxynucleotidyl transferase-positive (TdT+) leukemic cells. *Biochem. Pharmacol.* **2000**, *59* (3), 273−281.
(28) Kabsch, W. XDS. *Acta Crystallogr., Sect. D: Biol. Crystallogr.* **2010**, *66*, 125−132.
(29) Evans, P. R. An introduction to data reduction: space-group determination, scaling and intensity statistics. *Acta Crystallogr., Sect. D: Biol. Crystallogr.* **2011**, *67*, 282−292.
(30) Evans, P. R. Scaling and assessment of data quality. *Acta Crystallogr., Sect. D: Biol. Crystallogr.* **2005**, *62*, 72−82.
(31) McCoy, A. J.; Grosse-Kunstleve, R. W.; Adams, P. D.; Winn, M. D.; Storoni, L. C.; Read, R. J. Phaser crystallographic software. *J. Appl. Crystallogr.* **2007**, *40*, 658−674.
(32) Bricogne, G.; Blanc, E.; Brandl, M.; Flensburg, C.; Keller, P.; Paciorek, W.; Roversi, P.; Sharff, A.; Smart, O. S.; Vonrhein, C.; Womack, T. O. *BUSTER*, version 2.11.2; Global Phasing Ltd: Cambridge, U.K., 2011.
(33) Painter, J.; Merritt, E. A. Optimal description of a protein structure in terms of multiple groups undergoing TLS motion. *Acta Crystallogr., Sect. D: Biol. Crystallogr.* **2006**, *62*, 439−450.
(34) Emsley, P.; Cowtan, K. Coot: model-building tools for molecular graphics. *Acta Crystallogr., Sect. D: Biol. Crystallogr.* **2004**, *60*, 2126−2132.
(35) Schüttelkopf, A. W.; van Aalten, D. M. F. PRODRG: a tool for high-throughput crystallography of protein−ligand complexes. *Acta Crystallogr., Sect. D: Biol. Crystallogr.* **2004**, *60*, 1355−1363.
(36) Chen, V. B.; Arendall, W. B., III; Headd, J. J.; Keedy, D. A.; Immormino, R. M.; Kapral, G. J.; Murray, L. W.; Richardson, J. S.; Richardson, D. C. MolProbity: all-atom structure validation for macromolecular crystallography. *Acta Crystallogr., Sect. D: Biol. Crystallogr.* **2010**, *66*, 12−21.